forests

MDPI

Article

Unfolding the Roles of Particulate- and Mineral-Associated Organic Carbon in Soil Microbial Communities

Haiyan Sun [1,*], Fei Sun [1], Xiaoli Deng [2], Naleen Storn [2] and Shubo Wan [3]

[1] School of Economics and Management, Northeast Petroleum University, Daqing 163318, China; sunfeif@163.com
[2] Department of Soil Science of Temperate Ecosystems, Department of Agricultural Soil Science, University of Göttingen, 37077 Göttingen, Germany; xiaoli88@163.com (X.D.); stornna@gmail.com (N.S.)
[3] Shandong Academy of Agricultural Sciences, Jinan 265500, China; fhgreat@126.com
* Correspondence: haiyansun2025@163.com

Abstract: Forest succession is a rapid approach that can be used to increase soil carbon (C) stocks. It is crucial to understand how forest succession influences microbial community assembly and soil carbon fractions to improve carbon sequestration strategies. This present work analyzed microbial communities in forest succession, and the effects of particulate-associated organic C (POC) and mineral-associated organic C (MAOC) on microbial community structure and assembly in forest succession in Changbai Mountains, China. Compared to cropland, primary forest increased MAOC by 35% and POC by 43%, suggesting the importance of POC for microbial assembly processes, offering insights into forest restoration practices to enhance soil carbon sequestration. As succession proceeds, weak environmental selection facilitated the reduced deterministic processes, whereas local ecological and dispersal drift were elevated. Such shifts in fungal and bacterial communities could be mostly triggered by soil pH. Considering that POC was important, shifts in assembly processes can be determined by resource availability rather than succession sequences. Such findings conform to the neutral hypothesis, suggesting that POC exerts a negligible effect on analyzing microbial community assembly in forest succession. Overall, this present work sheds more light on the important effects of POC and MAOC on modeling different microbial communities and community assembly in forest succession.

Keywords: particulate organic carbon; mineral-associated organic carbon; microbial community; assembly processes; forest succession; high-throughput sequencing

Academic Editor: Anna Zavarzina

Received: 27 November 2024
Revised: 13 December 2024
Accepted: 23 December 2024
Published: 27 December 2024

Citation: Sun, H.; Sun, F.; Deng, X.; Storn, N.; Wan, S. Unfolding the Roles of Particulate- and Mineral-Associated Organic Carbon in Soil Microbial Communities. *Forests* **2025**, *16*, 27. https://doi.org/10.3390/f16010027

1. Introduction

Untroubled primary forests contribute to storing excessive soil organic carbon (SOC); thus, they are the important carbon sink that can mitigate climate change [1–3]. At present, an increasing number of primary forests are transformed into secondary forests, plantations, or additional land uses due to human activities and climate change [4–6]. Therefore, SOC storage is reduced and SOC stability and formation paths are changed, which have substantially affected SOC sequestration [1,2]. According to the latest frameworks, SOC deposition and maintenance, climate change response, and land management and utilization have been widely investigated by classifying SOC as particulate organic C (POC) or mineral-associated organic C (MAOC) [1,7–9]. POC consists of plant-derived structural polymers [10,11], including different structural compounds that have decreased N contents and defend against soil microbial attacks through the physical protection of aggregates and inherent biochemical resistance [12,13]. POC shows a decreased lifespan, with average

residence time between years and decades [14,15]. By contrast, MAOC mostly contains microbial products (high-/low-molecular-weight compounds) that have an increased N content, and it is persistent within soil because of chemical bonding with Ca, Mn, and Mg oxides, and macroaggregate-mediated physical protection [11,16–18]. Owing to the mineral protection, the mean residence time is between decades and centuries, and it is less susceptible to environmental disturbance and change than POC [15,19]. Nevertheless, the SOC fractions are usually neglected in research, limiting a comprehensive understanding of SOC deposition and susceptibility in forest transformation.

The microbial assembly processes remain a hotspot in microbial ecology because of its assistance in the mechanical knowledge of the drivers of community succession [20,21]. Microbial community assembly is mostly influenced by deterministic processes, confirming the "everything is everywhere, but the environment selects" principle [22,23]. However, stochastic processes must not be neglected in the case of dispersal events and random extinctions. Soil can store excessive SOC in forest succession, and SOC is a vital part of C input studies [24,25]. Microbial communities play an essential role in SOC cycling, directly or indirectly providing services to forest ecosystems [26]. The balance of microbial assembly processes may be strongly affected by soil C fractions [27]. The microbial community assembly collection process is expected to influence carbon metabolism-related microbial activities by limiting community membership, and it exerts a vital impact on POC and MAOC immobilization and mineralization [7,8]. For instance, in salt marsh plant community succession, SOC temporal alterations exert the most potent selection of bacterial community assembly [28]. Based on Luan et al. [29], the greatest carbon metabolic capacity can be obtained at the maximal selection pressure, with minimal dispersal. In this regard, microbial assembly processes may dominate the formation of SOC (especially POC and MAOC immobilization and mineralization). Thus, for understanding how forest succession affects microbial community and assembly, we should associate it with soil C fractions.

This present work was conducted in Changbai Mountains, China. Approximately 5 decades ago, some forests in this area were deforested, forming a large area of various forest succession stages [24]. Therefore, this area exhibits a good forest succession sequence to study microbial community succession patterns. Shifts in stochastic and deterministic balance may be linked to alterations in SOC fractions. Higher SOC can increase environmental heterogeneity through diversifying resource availability for soil microorganisms as well as plant–microorganism feedbacks, thereby enhancing deterministic selection [30,31]. To address these issues, through analyzing microbial communities in forest succession, we analyzed major effects of POC and MAOC on shaping microbial community assembly and structures in forest succession of Changbai Mountains, China. Unlike bulk SOC, POC and MAOC exhibit distinct turnover rates and stability, offering unique insights into microbial dynamics during succession. Thus, we hypothesized that: (1) deterministic processes dominate microbial assembly during early succession stages, and stochasticity increases later; (2) SOC fractions, particularly POC, explain differences in responses of microbial communities.

2. Materials and Methods

2.1. Study Site

We carried out the present work at the Research Station of Changbai Mountain Forest Ecosystem in Northeast China (42°23′ N and 128°50′ E) (Figure S1). This site shows a representative continental temperate monsoon climate, and altitude, mean annual temperature, and precipitation are 780 m, 4.1 °C, and 840.3 mm, respectively. The soils can be classified as dark brown soil (Chinese soil taxonomy) or Alfisol (USDA soil taxonomy), bedrocks are

volcanic ash and weathered basalt, and maximum soil layer depth is 10 m. Table S1 shows vegetation featured at this site.

2.2. Sampling

Field samples were collected in September 2024, with forest succession (secondary forest succession referred to woody vegetation regrowing following total forest clearance for human activities, and primary forests are primary or old-growth forests without clear-felling and are slightly or not affected by known recent human disturbance [32]) being chosen: primary forest (PF), secondary forest (SF), as well as cropland (CL), common land-use types of dryland cultivation (for corn) adopted in the last 50 years. SF and CL are transformable based on PF with the same background [33]. We selected five plots (around 50 × 50 m) of each forest type at a mutual distance of 50–100 m [34]. We randomly chose 15 subplots (1 × 1 m) of each plot. Litter and rock were removed to obtain surface samples. Totally, we obtained 5 (depth, 0–20 cm) random soil cores (diameter, 5.5 cm), with each layer mixed within one plot for forming a mixture sample. Altogether, we obtained 225 soil samples (three land conversion types × five replicates × 15 samples). Thereafter, we further divided fresh soil samples in two subsamples, one for preservation under 4 °C to analyze physicochemical characters, and one for preservation under −80 °C for microbial DNA analysis.

We performed a field survey at peak growing season from July to August in 2024. Vegetation coverage was estimated in each plot, and the *Pi* was calculated [15]:

$$Pi = \mathrm{i}/Ti$$

i stands for specific sample species, and *Ti* represents overall sample species; *Pi* demonstrates importance value.

The plant diversity (Shannon–Wiener index) uses the information-theoretic method for predicting species that the subsequently harvested individual belonged to. For the larger community species diversity, there was a higher uncertainty in subsequent individual prediction. The equation below was adopted for calculation:

$$\mathrm{H} = -\sum_{i=1}^{\mathrm{s}} Pi \ln Pi$$

S represents species number and *Pi* indicates importance value.

2.3. Analyses of Soil Physicochemical Characters

We utilized a pH meter (ThermoFisher Scientific Inc., San Jose, CA, USA) for analyzing soil pH with aqueous suspension (soil:water = 1:5, w/v). Later, 10 g fresh samples were dried for a 48 h period under 105 °C to constant weight for measuring soil moisture content by means of gravimetry. Soil organic matter (SOM) was analyzed with the potassium dichromate oxidation method (Six and Paustian, 2014). Through using the 0.58 conversion factor, we analyzed SOC level (g kg^{-1}) according to SOM. Soil total phosphorus and nitrogen (TP and TN, g kg^{-1}) were analyzed through colorimetry, Kjeldahl, and molybdenum antimony (Bremner, 1960). Absorbance was measured at 660 nm with a spectrophotometer (FLUOstar Omega, BMG Labtech, Ortenberg, Germany). The chloroform fumigation–extraction process was utilized for analyzing soil microbial biomass C, P, N (MBC, MBP, and MBN, mg kg^{-1}) [35]. Each sample was analyzed thrice to take the average as the final result. Table S2 displays soil physicochemical properties.

We adopted compounds that give great fluorescence, such as 4-methylumbelliferone (MUB) and 7-amino-4-methylcoumarin (MUC), to measure soil extracellular enzymes,

such as acid phosphatase (AP), α-1,4-glucosidase (AG), and β-N-acetylglucosaminidase (NAG) by fluorometry. Thereafter, we drew standard curves of MUB and MUC (0, 2.5, 5, 10, 25, 50, and 100 mL) [36]. Around 4 g freshly collected samples were stirred for a 2 min period in 40 mL acetic acid buffer solution (pH 5.0) for forming homogenate. Afterwards, 100 mL homogenate was added with 150 mL buffer, and the mixture was added in a microtiter plate. We set one test (substrate + homogenate) along with one control (buffer + homogenate) sample of every sample. The 96-well microplates were incubated for a 3 h duration under 25 °C, and later, 1 mL of 1 M NaOH was added for terminating reactions, thus analyzing soil extracellular enzymes, which were expressed as nmol activity g^{-1} dry soil h^{-1} (nmol $g^{-1}h^{-1}$) after quenching was corrected. We detected fluorescence intensity at 365 and 450 excitation and emission wavelengths, respectively. Table S2 displays enzyme substrates, commissions, and incubation duration.

2.4. Soil POC and MAOC

Soil organic C could be categorized as POC or MAOC by wet sieving and particle-size fractionation. In brief, air-dried soil samples (20 g) were added to the 50 mL plastic bottles that contained 5% (w/v) sodium hexametaphosphate solution. Thereafter, we put bottles onto the shaker for 2 h agitation at 180 rpm for complete blending, and later spread the soil homogenates using the reciprocal sieve shaker (AS200 control, Retsch, Germany) by the 53 μm sieve, and subsequently dispersed them using deionized water. Afterwards, this shaker underwent movement 3 cm up and down 100 times. Meanwhile, we added deionized water into this sieve persistently for facilitating organic matter dispersion in aggregates. Then, the fractions remaining on and crossing this sieve were dried in the beaker at 60 °C prior to weighing. Finally, two fractions including POC (>53 μm) and MAOC (<53 μm) could be obtained.

2.5. DNA Extraction and Bioinformatics Analysis

We extracted total soil microbial DNA by the cetyltrimethylammonium bromide approach. We also profiled fungal and bacterial communities through targeting ITS1 and V4–V5 regions within 18S and 16S rRNA genes, respectively [37]. PCR was performed to amplify target sequences using ITS5-1737F/ITS2-2043R and 515F/907R primers for fungal and bacterial communities, respectively. Sequencing was completed with the Nova Seq 6000 platform (Illumina Inc., San Diego, CA, USA). By adopting the DADA2 module of QIIME2 (Version QIIME2-202006), read assembly in amplicon sequence variants (ASVs) was conducted after quality filtering. Unite and Silva Databases were adopted for annotations of fungi and bacteria, respectively [38]. Furthermore, sequencing results were imported into the National Center for Biotechnology Information Sequence Read Archive database (accession number PRJNA1022345 and PRJNA1023123).

2.6. Microbial Community Assembly

We utilized alpha-diversity indices for evaluating microbial communities, and null models for assessing the contributions of selection and dispersal processes to community turnover [39]. Therefore, we analyzed phylogenetic beta-diversity (β-nearest taxon index, βNTI) and taxonomic indices, and later determined the alterations by the Bray–Curtis-based Raup–Crick metric (RCbray) [40]. βNTI indicates if deterministic processes occupy the dominance, accompanied by unexpected significantly decreased (homogeneous selection: $\beta NTI < -2$) or increased (variable selection: $\beta NTI > 2$) phylogenetic transitions. Notably, $|\beta NTI| < 2$ and $RCbray < -0.95$ demonstrate markedly increased species quantities within two communities relative to occasional expectation (homogeneous dispersal), while $RCbray > 0.95$ indicates markedly decreased species quantities within two communities relative to occasional expectation (dispersal limitation). Moreover, upon $|RCbray| < 0.95$,

the two communities show the maximal shared species under occasional expectation, suggesting the only "non-dominant" component (drift) [28].

2.7. Co-Occurrence Network Analysis

"WGCNA" package in R (V4.1.2) was utilized for building microbial networks [41]. *p*-value adjustment was completed using Benjamini and Hochberg false discovery rates [42]. This study only employed ASVs whose relative abundance was >0.001 in analysis. Statistical correlation was identified upon $p < 0.05$ and Pearson's $r > 0.7$, and these standards were later adopted in co-occurrence network construction [43]. Network topological features were determined with "igraph" in R [44]. Network complexity was evaluated using node/edge numbers and average degree value, with greater node/edge quantities and higher average degree value representing the higher network complexity [45]. 'mixOmics' in R was adopted for computing value importance in projection (VIP) for partial least squares (PLS) regression [46]. Moreover, it was the predicting factor for assessing importance of ASV occurrence within this network for βNTI. Typically, we chose ASVs that had great degrees (5 most significant within this network) and VIP (>1) to be keystone taxa. Network was visualized by Gephi software (V0.10.1).

2.8. Statistical Analysis

We used SPSS23.0 (IBM, Armonk, NY, USA) to carry out Fisher's test and one-way ANOVA upon the thresholds of 95% and 99% confidence intervals (CIs), respectively ($p < 0.05$ and $p < 0.01$). The Circos plot was used for visualizing microbial phylum's taxonomic distribution in different succession stages by adopting R software (V4.1.2). Simultaneously, "vegan" of R was adopted to determine microbial community alpha-diversity [47]. Moreover, QIIME 2 software (Version QIIME2-202006) was employed for analyzing the Bray–Curtis measure of dissimilarity in microbial communities, with result visualization being conducted using nonmetric multidimensional scaling (NMDS) by "metaMDS" function of R package "vegan" [48]. For obtaining reliable NMDS results, we performed significance tests with nonparametric multivariate ANOVA (Adonis) and analysis of similarities (ANOSIM). We utilized NMDS scores for first axis for representing structures of fungal and bacterial communities. This study carried out linear regression for analyzing associations of POC and MAOC with microbial community and assembly processes through R package "ggplot2". Moreover, we adopted Pearson's correlation analysis for evaluating associations of keystone taxa, POC, and MAOC, together with microbial community assembly, with "corrplot" in R package [49]. At last, we adopted AMOS (V 21.0) (https://sourceforge.net/projects/amos/) (accessed on 22 December 2024) to construct structural equation models (SEM) to illustrate how POC and MAOC influence microbial community assembly.

3. Results

3.1. Soil POC, MAOC, and Microbial Composition in Forest Succession

Relative levels of POC and MAOC were different during forest succession (Figure 1, $p < 0.05$). In forest succession, POC and MAOC levels gradually increased. There are significantly differences across forest succession. According to the 97% sequence similarity level, saturated rarefaction curves were smoothed (Figure S2). Differences in fungal and bacterial strains were detected, accompanied by aggregated distribution in forest succession (Figure 2). Clustering of soil fungal and bacterial strains was completed into diverse ecosystems (Figure 2). To be specific, we classified soil bacterial sequences into 13 phyla upon 97% similarity (Table S4), and dominant phyla included *Actinobacteria*, *Proteobacteria*, and *Acidobacteria* (relative abundances > 5%), taking up 70%

of total sequences. Additionally, we classified soil fungal sequences into eight phyla upon 97% similarity (Table S5), and dominant phyla included *Ascomycota*, *Basidiomycota*, and *Chytridiomycota* (relative abundances > 5%), taking up 70% of total sequences. Fungal and bacterial species had slowly increased Shannon–Wiener indices during forest succession (Table S5). Compared to the cropland, *Actinobacteria* had gradually declined relative abundance in forest succession. Nonetheless, *Proteobacteria* and *Acidobacteria* exhibited slowly increased relative abundances in forest succession (Figure 2). Apart from soil fungal species, *Ascomycota* and *Basidiomycota* had increased and declined relative abundances in forest succession, respectively (Figure 2).

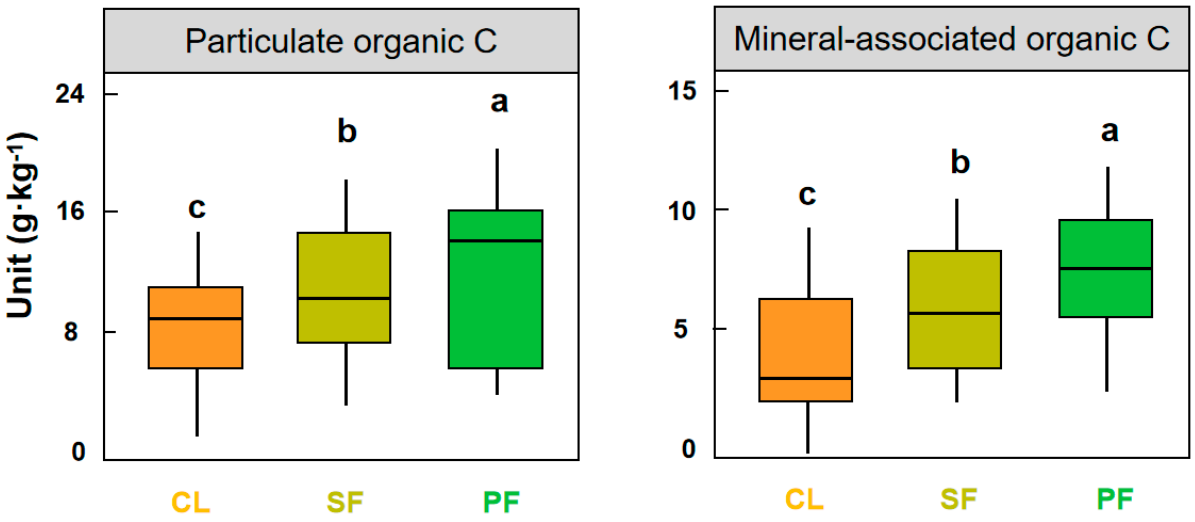

Figure 1. Particulate and mineral-associated organic carbon during forest succession. One-way ANOVA was adopted for testing between-succession heterogeneities with one sample *t*-test. Horizontal bars inside boxes indicate medians. Box tops and bottoms stand for 75th and 25th percentiles, respectively. Letters are indicative of significant differences ($p < 0.05$) among forest successions. Primary forest (PF), secondary forest (SF), and cropland (CL).

The present work utilized a taxon–taxon co-occurrence network to visualize complex microbial community networks in forest succession (Figure 3). Thus, PF had larger microbial communities as well as greater average node connectivity degrees (in terms of node/edge numbers) (Figure 3). Microbial communities within PF had remarkably increased node connectivity degrees as well as integrated positive (85.8%) and negative (14.2%) connections. PF had an average microbial connectivity degree of clustering coefficient of PF increased, suggesting a lower community network complexity with increasing environmental stress.

3.2. Soil Microbial Assembly in Forest Succession

βNTI was used to analyze how forest succession affected microbial assembly according to phylogenetic tree and community abundance data in forest succession. Consequently, deterministic processes ($|\beta NTI| > 2$), especially homogeneous selection, exerted a key effect on fungal and bacterial community assembly at two depths (Figure 4). Relative to PF, microbial communities in CL showed lower deterministic assembly processes. The stages of succession suggested the gradual alteration of βNTI in forest succession, and strongest deterministic assembly could be observed from PF relative to others. Nonetheless, stochastic assembly processes had vital impact, while deterministic assembly processes of CL were gradually weakened. On the whole, in later succession, deterministic processes (homogeneous selection) of microbial communities became weaker than those in early

succession (Figure 4). Drift and dispersal limitations had important effects on fungal and bacterial stochastic processes in forest succession.

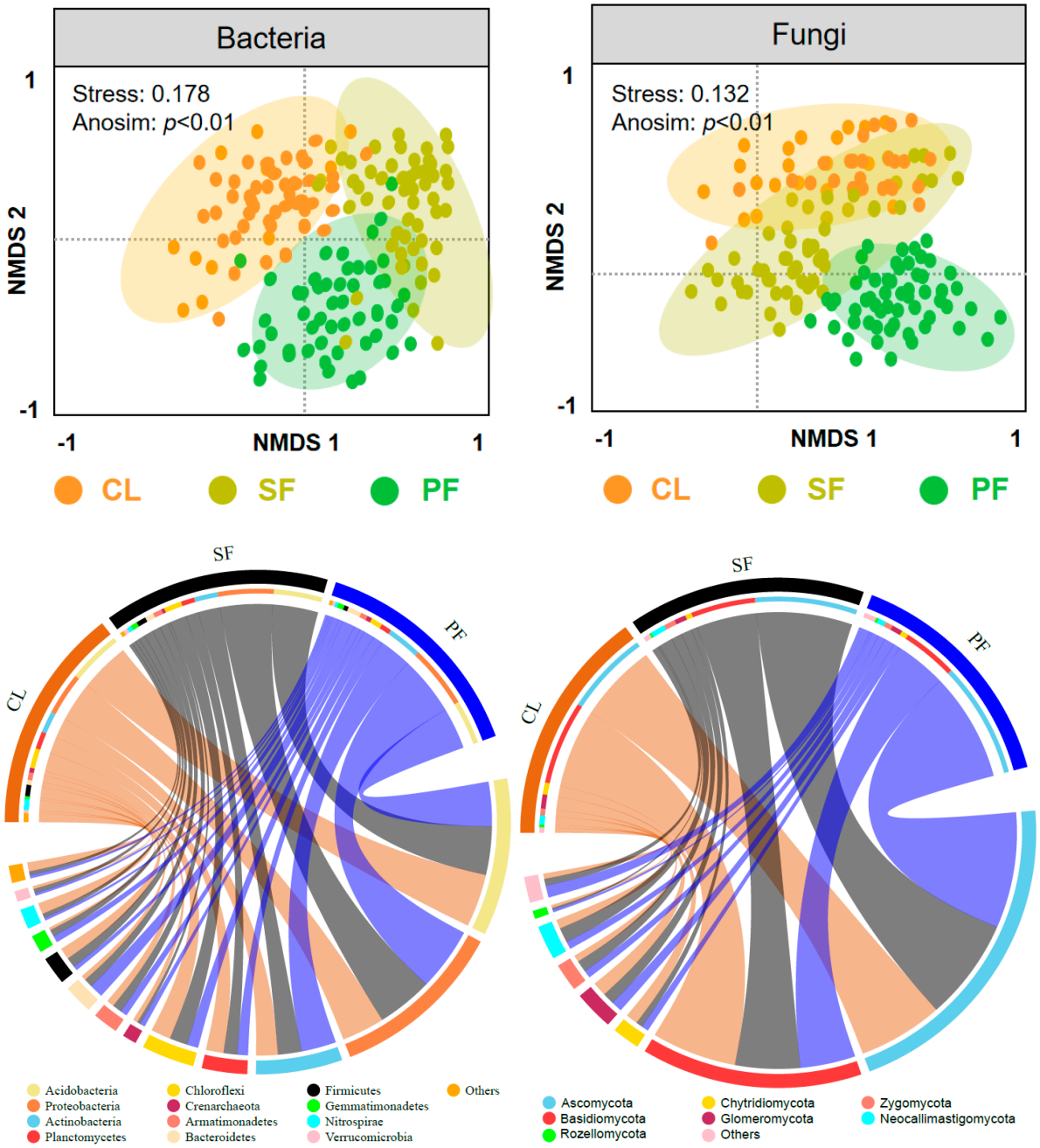

Figure 2. Predominant phylum relative abundances in forest succession. Microbial beta-diversity in forest succession. ANOSIM *p* was adopted for testing if between-group differences markedly increased relative to within-group differences, thus determining the significance of grouping. Primary forest (PF), secondary forest (SF), and cropland (CL).

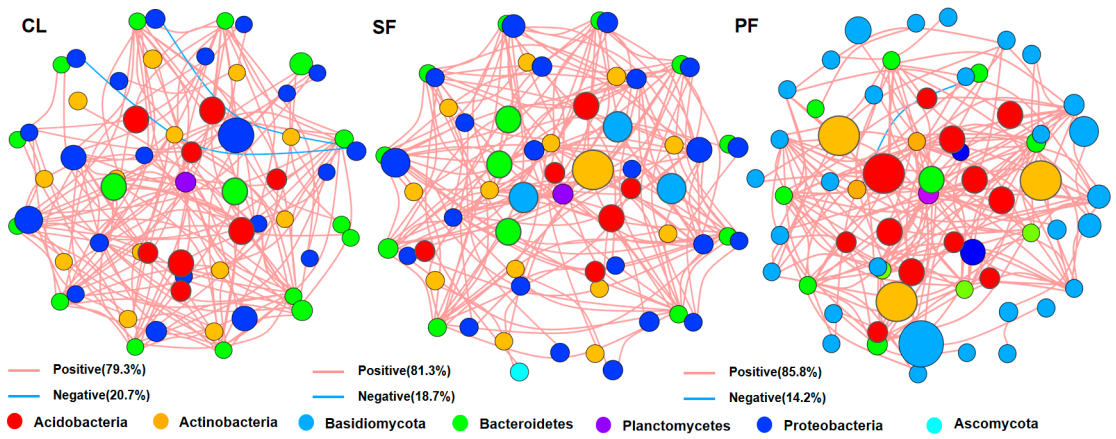

Figure 3. Microbial community cross-kingdom co-occurrence network in forest succession. Colors in this network indicate different phyla. The node size (ASVs) is in direct proportion to connection number. Nodes with mutual significant ($p < 0.05$) and strong correlation (Spearman's > 0.7) were linked (edges). Edge thickness is in direct proportion to Spearman's correlation coefficients. Red edges stand for positive connections, whereas green edges represent negative interactions. Primary forest (PF), secondary forest (SF), and cropland (CL).

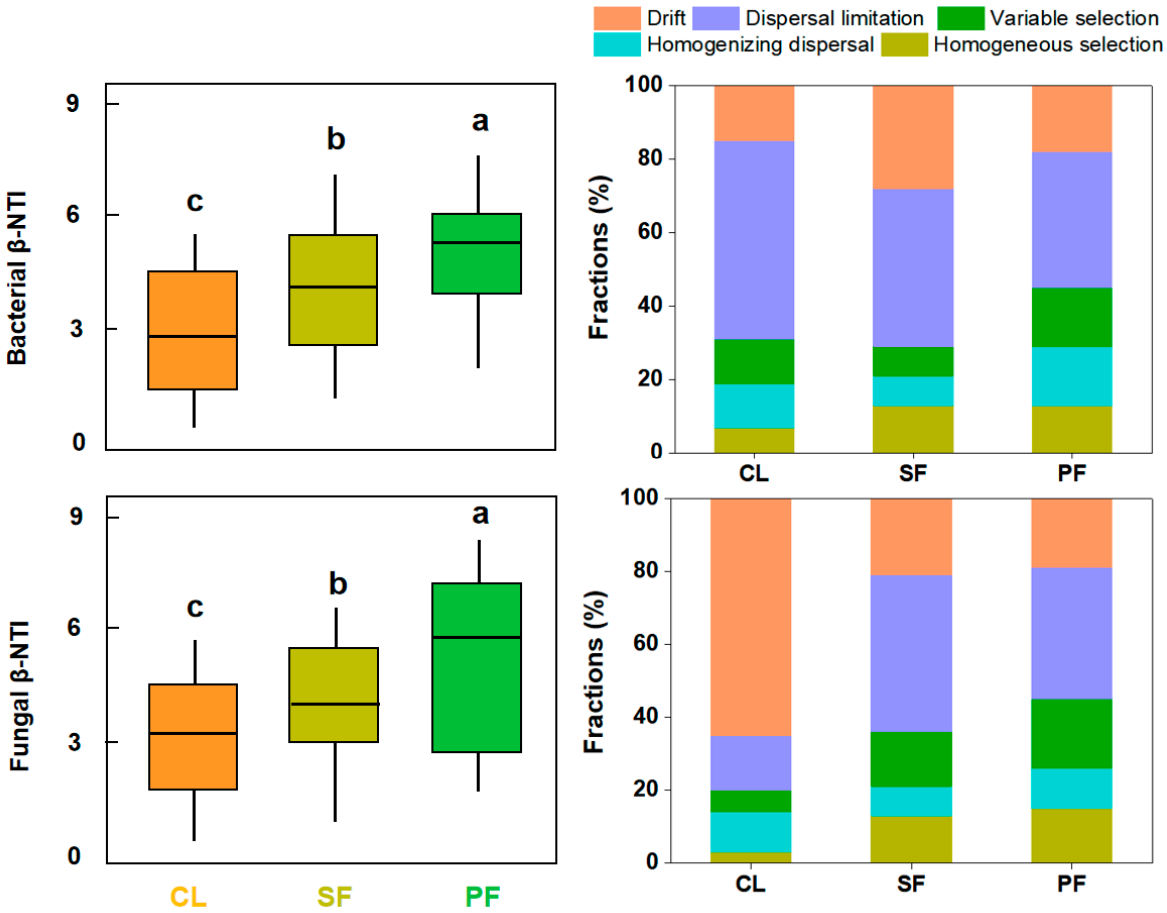

Figure 4. Microbial β-NTI distribution to conduct pairwise comparisons of communities. Horizontal bars inside boxes stand for medians. Box tops and bottoms stand for 75th and 25th percentiles, respectively. Letters are indicative of significant differences ($p < 0.05$) among forest succession. Primary forest (PF), secondary forest (SF), and cropland (CL).

3.3. Links Between POC, MAOC, and Microbial Community

Linear regressions showed strong associations between POC, MAOC, and assembly of microbial communities (Figure 5). Pearson analysis revealed that SOC fractions were positively related to microbial community (Figure 6). Moreover, *Acidobacteria* relative abundance exhibited positive association with POC, and negative correlation with MAOC. The Proteobacteria relative abundance showed negative association with POC. *Ascomycota* and *Basidiomycota* exhibited positive correlation with MAOC. Furthermore, POC potently suggested alterations in microbial community assembly relative to MAOC. Soil pH is the main driving factor related to microbial communities.

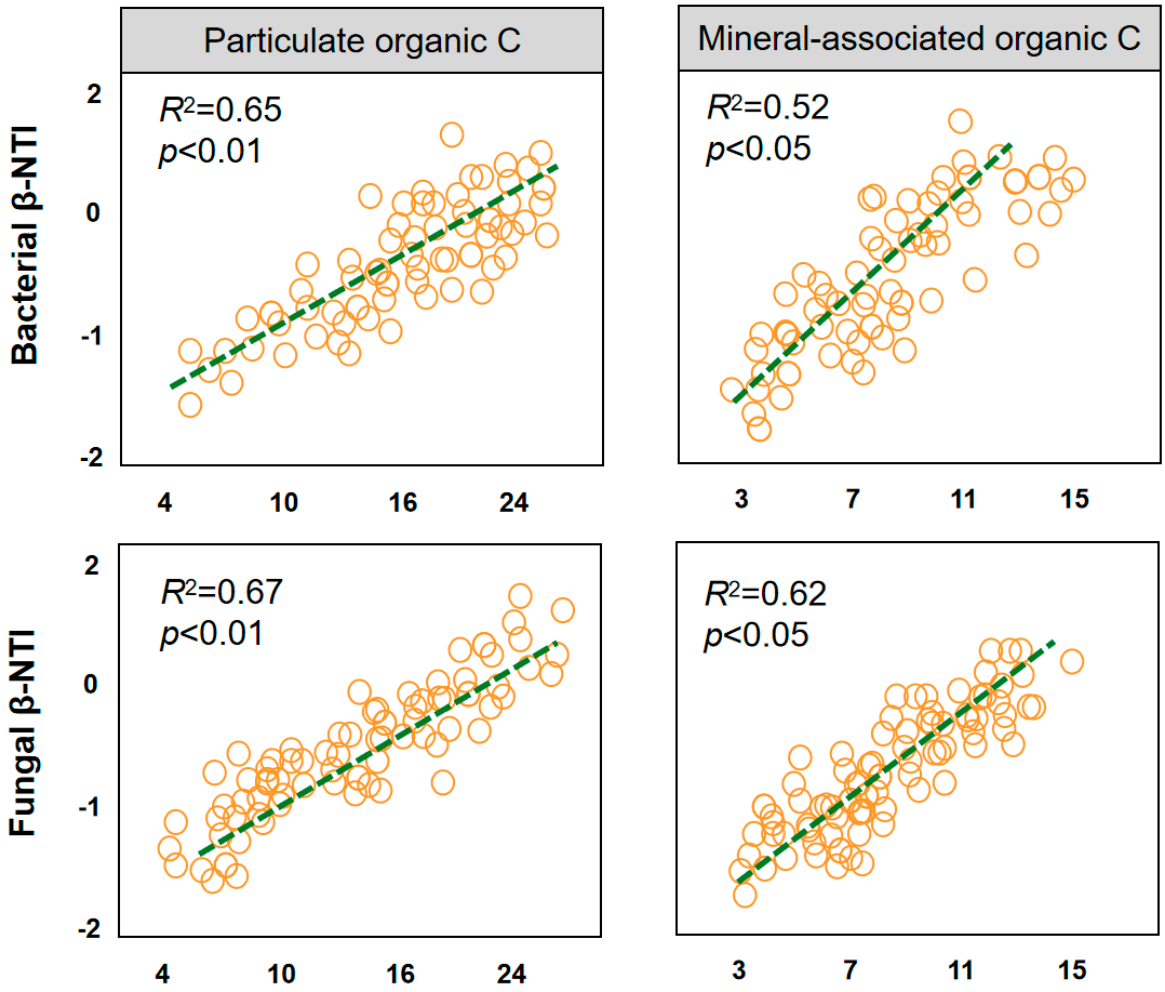

Figure 5. Linear regressions between POC, MAOC, and microbial community assembly processes. Regression significance level was set at $p < 0.011$. p and R^2 were determined with the distance-based linear regression model.

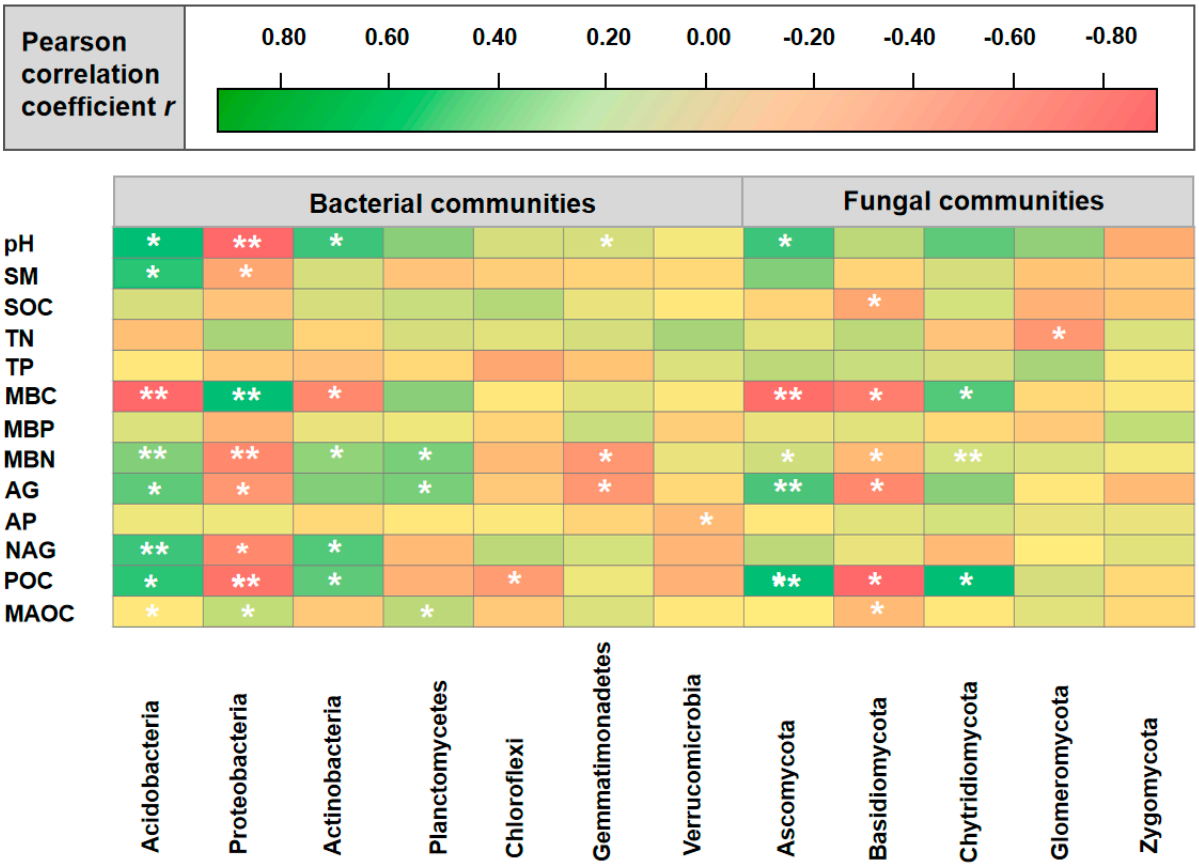

Figure 6. Pearson correlations between the relative abundance of the dominant microbial phyla and soil carbon fractions. The orange color indicates negative correlations, while the green color indicates positive correlations (dark orange, $r = -0.80$, dark green, $r = 0.80$), with correlation coefficients (Perason ρ) represented by the scale to the right. *, $p < 0.05$; **, $p < 0.01$. SM: soil moisture; TN: soil total nitrogen; TP: soil total phosphorus; MBC: soil microbial biomass carbon; MBN: soil microbial biomass nitrogen; MBP: soil microbial biomass phosphorus; AG: α-1,4-glucosidase; AP: acid phosphatase; NAG: β-N-acetylglucosaminidase.

SEM was performed to determine SOC fractions' regulation of microbial community assembly (Figure 7 and S3). We put forward the final SEM by adopting a knowledge-based priori model, depicting relevant flows regarding the causal relations of environmental variables with microbial community assembly. Following SEM, forest succession negatively affected MAOC, but positively affected POC. More specifically, MAOC negatively affected fungal community assembly, while POC positively affected bacterial community assembly.

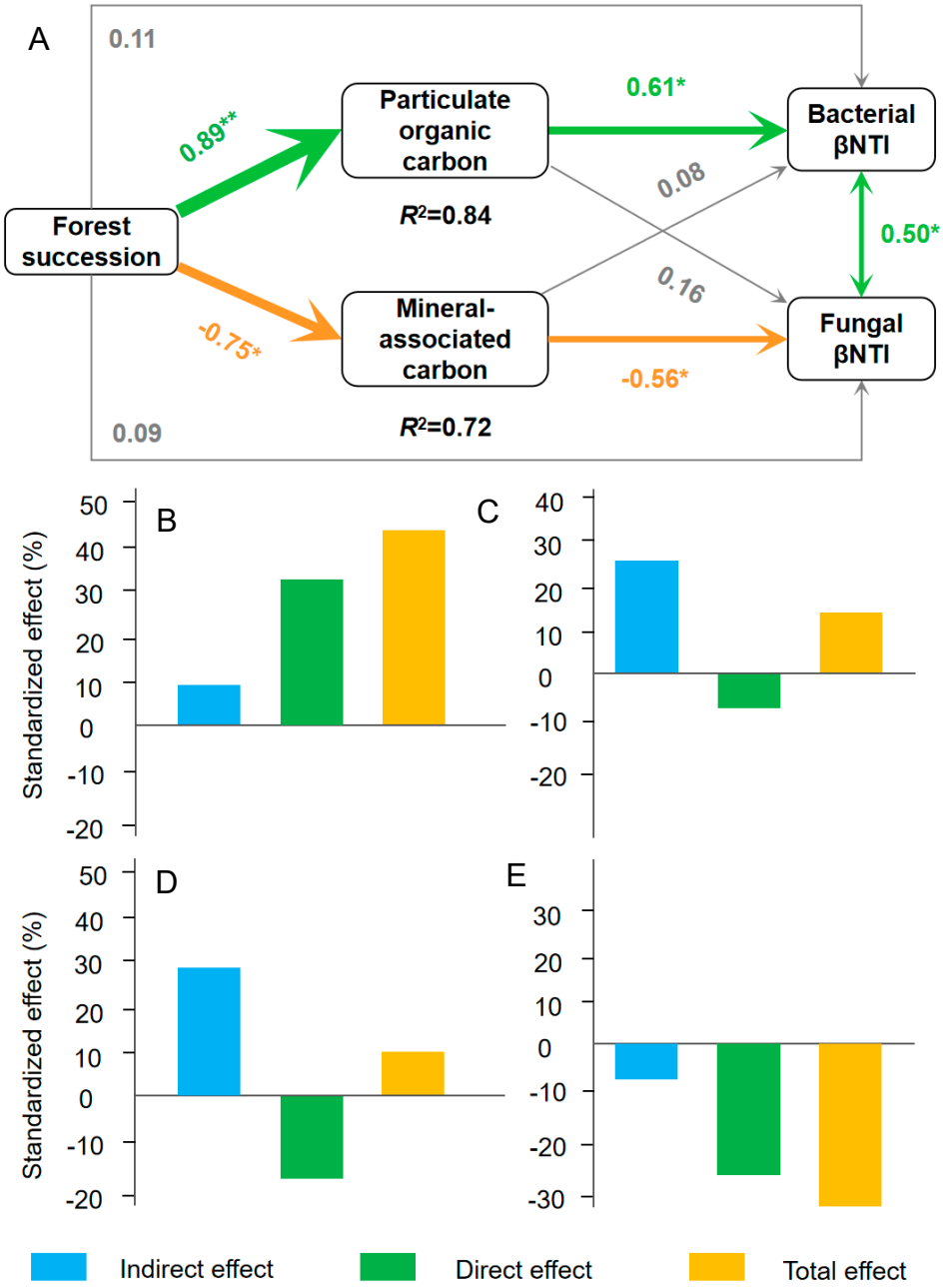

Figure 7. Structural equation model (**A**) depicting soil carbon fractions' direct and indirect effects ((**B**,**C**) POC and MAOC effects on bacterial assembly processes; (**D**,**E**) POC and MAOC effects on fungal assembly processes) on microbial community assembly (p = 0.03, χ^2 = 7.65, CFI = 0.98, AIC = 198.1, RSMEA = 0.001, 89.5% explained variation). Green and orange arrows stand for remarkably positive and negative pathways, respectively. Data near arrows represent standardized path coefficients, which are close to relative regression weights, and indicate size effect on relationship. Arrow thickness is in direct proportion to covariation coefficient or standardized path coefficient magnitude. R^2 was determined following 999 bootstraps, representing variance interpreted percentage of every dependent variable within this model. * $p < 0.05$, ** $p < 0.01$.

4. Discussion

4.1. Soil POC and MAOC During Forest Succession

Many articles support the first hypothesis that POC substantially increases after forest succession [7,50]. This is because that POC contains different structural compounds that have decreased N contents, thus resisting soil microbial attacks via physical protection

and internal biochemical resistance within aggregates [51]. Therefore, the POC was higher than MAOC during forest succession (Figure 1). In forest succession, plant biomass-derived primary C (mostly below-ground) input in POC increases, causing the deposition of POC [51,52]. Based on Six et al. [53], POC exerted its physical protection through SOC sequestration. As reported by Garcia-Franco et al. [54], soil aggregation associated with changes in microbial communities modulated SOC sequestration after semi-arid shrubland afforestation. Forest succession may result in fast and excess macroaggregate generation [55], leading to POC protection and deposition [18,51]. Different from POC, MAOC, the mineral matrix-related stable SOC pool, exhibits greater physical protection and is less susceptible to mineralization [1,8,16]. In some studies, MAOC increases owing to vegetation restoration [18,56,57]. Likewise, the MAOC level increases in forest succession (Figure 1). Relative to the increased POC ratio, labile POC shows higher sensitivity to grassland restoration than MAOC, demonstrating the second hypothesis.

4.2. Microbial Diversity and Composition in Forest Succession

Alpha-diversity indicators (Chao and Shannon indices) slowly increased in forest succession (Tables S4 and S5), suggesting furious microbial community competition for resources in later forest succession. Competition can enhance species diversity, which also causes the increased diversity during later forest succession [33]. Such findings are consistent with previous reports in diverse ecosystems [31,33,34]. As confirmed by null deviation analysis and neutral community modeling results, stochastic and selection changes had a key role in ecosystem recovery, resulting in the community structural trajectory succession [58]. When heterogeneities of microbial diversity, richness, and main species in forest succession were identified, this work examined the taxon–taxon co-occurrence network for dealing with complex associations among microbial communities (Figure 3). Consequently, the microbial community co-occurrence network of PF exhibited increased complexity compared with CL. Typically, PF had greater resources, causing a greater ASVs co-occurrence degree of diverse modules. Given the growing node/edge quantities, modularity and negative correlation ratios in succession, this microbial network was stable and complex in later succession. In addition, a higher modularity revealed that this network was more stable by limiting the role of taxa loss in communities [59].

4.3. Microbial Assembly Processes in Forest Succession

Here, Acidibacter and Ascomycete (the dominant microbes) are acid-tolerant and suitable in acidic soils, and pH was significantly different during forest succession. Both Acidibacter and Ascomycete were strongly linked to soil pH (Figure 6). Soil pH might affect microbes by selective pressure on fitness and survival of soil microorganisms under strongly acidic soil conditions in tested forests [58]. The succession increased soil pH, whereas microbial communities were under the negative impact of soil pH since many bacterial taxa have narrower growth tolerances [21]. In addition, soil pH is a rigid environmental filter causing phylogenetic clustering, despite successional age, which has been recognized as an important abiotic factor for community assembly [50,51]. Therefore, there was a large pH difference among different succession stages ($p < 0.05$) (Table S3), and this may induce the gradual shift from deterministic to stochastic processes.

Our observed dominance of deterministic processes during early succession aligns with our hypothesis, and suggests strong environmental filtering during initial community establishment. Determinism greatly affected fungal community assembly in early succession (Figure 4), while stochasticity became predominant in later succession, conforming to previous findings [31,60,61]. Plant community composition markedly affects fungal communities [62]. Due to the close relation of fungi with plants, like mutualism, alterations

in plant composition directly affect fungi as the strong filters, causing the different fungal communities [63]. Additionally, plants may indirectly affect fungi, inducing alterations in fungal communities in succession via heterogeneous litter biochemistry [20]. Following niche-based theory, deterministic processes are dominant in community structure. The strong deterministic processes in the case of poor available resource and extreme environmental conditions are common, which is the greater determinism (low βNTI) in early succession [64]. Early stages had diverse plant community proportions in succession. Consequently, the role of plant community-induced fungal assembly processes is related to selection pressure (for example, low nutrient resources leads to higher symbiont proportion) on soil fungal fitness and survival in different plant communities within our analyzed forests during early succession; therefore, deterministic processes have relative importance in modulating fungal community structure [65,66]. However, the plant community becomes stable in later succession, thereby promoting environmental homogeneity [67]. Stochastic processes modeling fungal community structure in late succession are crucial to ecosystems within a homogenous environment [68,69]. Based on macroecological theory, stochasticity shows more and more relative impact according to resource availability, because nutrient supplement enhances stochastic processes and decreases niche selection [64,66]. As succession proceeds, alterations of plant communities may result in higher nutrient availability, including the higher SOC in later succession, therefore suppressing symbiotic fungus–plant relations [65,70]. Such results can promote stochastic processes to remodel fungal communities in later succession.

4.4. Linking POC and MAOC with Microbial Community Assembly

Carbon resource availability might affect microbial community assembly, and the latter was examined through the changing environment in forest succession (Figures 5 and 6). Alterations of the determinism–stochasticity balance are related to alterations in soil carbon fractions [58,71]. Higher SOC might promote environmental heterogeneity through increasing available resource diversity for soil communities and plant–microorganism feedbacks, which can thus enhance deterministic selection [72]. Thus, we further discussed the relation of microbial composition with POC and MAOC (Figure 5), finding that microbial communities were significantly positively or negatively related to different SOC compositions (Figure 6). SOC composition changed during forest succession, leading to heterogenous resource availability. It induced alterations in community and species structures, as well as microbial diversity, affecting microbial assembly [58,71]. As indicated by Pearson correlation, Actinobacteria was markedly positively related to methyl carbon (Figure 6). However, Acidobacteria was negatively related to methyl carbon, which might be related to microbial affinity for diverse carbon sources. Soil microbial communities may be mostly associated with labile SOC that is tightly linked with microbial taxa, and is ready for microbial mineralization, which indicates alterations in early soil C pools [21,73]. Thus, it mostly affects microbial communities. Consequently, long-time vegetation succession increases microbial network complexity and stability. Additionally, microbial community networks are mostly associated with labile SOC. This is because that soil microbial metabolic growth requires a lot of available nutrients and labile SOC; Thus, the structure of the microbial network is more complex in sufficient nutrients [72].

We utilized SEM to investigate microbial assembly mechanisms during long-time succession (Figure 7). POC accounted for a main driving factor for microbial community assembly, more than MAOC, confirming the second hypothesis. MAOC negatively affected fungal community assembly, while POC positively affected bacterial community assembly. It may be because that POC is ready for microorganisms to use, and influences the community composition and structure [21,73]. Key taxa are important controllers of

community assembly because they greatly affect microbial communities as the tightly related microorganisms [74,75]. For instance, key taxa showed a positive relation with βNTI, confirming these results. Overall, this work sheds more light on relations between microbial communities and labile SOC at a long-time scale. Thus, we consider that primary forest recovery could optimize POC and MAOC contributions to long-term carbon sequestration.

5. Conclusions

This work comprehensively analyzes the drivers, assembly mechanisms, and alterations of microbial community ecological functions during forest succession. Forest succession changes compositions and structures of bacterial and fungal communities, which are related to possible functional changes. Additionally, forest succession enhances the dispersal limitation processes in bacterial communities, but weakens fungal communities. Stochastic processes are crucial to model bacterial community assembly in succession, whereas deterministic processes are predominant during fungal community assembly, and stochastic selection slowly increases during succession. The POC and MAOC drive microbial assembly by influencing microbial keystone taxa, which provide new targeted treatment and indicators of the soil microenvironment. Consequently, future studies can measure critical taxa by metatranscriptomic and metagenomic approaches.

Supplementary Materials: The following supporting information can be downloaded at: https://www.mdpi.com/article/10.3390/f16010027/s1, Table S1. Characteristics of vegetation of study sites during forest succession. Table S2. Extracellular enzymes, assayed from soil samples, and their abbreviations used in this study, enzyme commission numbers, corresponding substrates, and incubation times. Table S3. Soil physical and chemical characteristics during forest succession. Table S4. Illumina MiSeq sequenced bacterial data and diversity indices (at 97% sequence similarity) based on the 16S gene for grassland sites with year since forest succession. Table S5. Illumina MiSeq sequenced fungal data and diversity indices (at 97% sequence similarity) based on the ITS rRNA gene with year since forest succession. Figure S1. Map showing the location of the study area. Figure S2. Rarefaction curves of sequence number at 97% similarity: A, soil bacterial community; B, soil fungal community. Figure S3. The index of co-occurrence network microbial communities during forest succession. The horizontal bars within boxes represent medians. The tops and bottoms of boxes represent the 75th percentiles and 25th percentiles, respectively. Letters indicate significant differences ($p < 0.05$) among forest succession. * $p < 0.05$, ** $p < 0.01$. Primary forest (PF), secondary forest (SF), and cropland (CL). Figure S4. The prior models depicting the effect of POC and MAOC on microbial community assembly processes.

Author Contributions: H.S.: conceptualization, data curation, software, visualization, writing—original draft. F.S.: investigation, funding acquisition, writing—original draft. X.D.: conceptualization, writing—review and editing. N.S.: conceptualization, supervision, writing—review and editing. S.W.: conceptualization, supervision, writing—review and editing. All authors have read and agreed to the published version of the manuscript.

Funding: The present work was supported by the Chinese Social Sciences Fund: Research on mechanism analysis, efficiency measurement, and path exploration of digital enabling low-carbon transformation on traditional energy industry (22BTJ046).

Data Availability Statement: All datasets used in the present work are available at online repositories. The repository/repositories names and accession number(s) are available at: https://www.ncbi.nlm.nih.gov/ (accessed on 5 January 2024), PRJNA1022345 and PRJNA1023123.

Conflicts of Interest: The authors declare that they have no known competing financial interests that could have influenced the work reported in this paper.

References

1. Lugato, E.; Lavallee, J.M.; Haddix, M.L.; Panagos, P.; Cotrufo, M.F. Different climate sensitivity of particulate and mineral-associated soil organic matter. *Nat. Geosci.* **2021**, *14*, 295–300. [CrossRef]
2. Beillouin, D.; Cardinael, R.; Berre, D.; Boyer, A.; Corbeels, M.; Fallot, A.; Feder, F.; Demenois, J. A global overview of studies about land management, land-use change, and climate change effects on soil organic carbon. *Glob. Change Biol.* **2022**, *28*, 1690–1702. [CrossRef]
3. Georgiou, K.; Jackson, R.B.; Vindušková, O.; Abramoff, R.Z.; Ahlström, A.; Feng, W.; Harden, J.W.; Pellegrini, A.F.A.; Polley, H.W.; Soong, J.L.; et al. Global stocks and capacity of mineral-associated soil organic carbon. *Nat. Commun.* **2022**, *13*, 3797. [CrossRef] [PubMed]
4. Elias, F.; Ferreira, J.; Lennox, G.D.; Berenguer, E.; Ferreira, S.; Schwartz, G.; Barlow, J. Assessing the growth and climate sensitivity of secondary forests in highly deforested Amazonian landscapes. *Ecology* **2020**, *101*, e02954. [CrossRef]
5. Matos, F.A.; Magnago, L.F.; Aquila Chan Miranda, C.; de Menezes, L.F.; Gastauer, M.; Safar, N.V.; Schaefer, C.E.G.R.; da Silva, M.P.; Simonelli, M.; Edwards, F.A.; et al. Secondary forest fragments offer important carbon and biodiversity cobenefits. *Glob. Change Biol.* **2020**, *26*, 509–522. [CrossRef] [PubMed]
6. Heinrich, V.H.; Dalagnol, R.; Cassol, H.L.; Rosan, T.M.; de Almeida, C.T.; Silva Junior, C.H.; Campanharo, W.A.; House, J.I.; Sitch, S.; Hales, T.C.; et al. Large carbon sink potential of secondary forests in the Brazilian Amazon to mitigate climate change. *Nat. Commun.* **2021**, *12*, 1785. [CrossRef]
7. Cotrufo, M.F.; Ranalli, M.G.; Haddix, M.L.; Six, J.; Lugato, E. Soil carbon storage informed by particulate and mineral-associated organic matter. *Nat. Geosci.* **2019**, *12*, 989–994. [CrossRef]
8. Lavallee, J.M.; Soong, J.L.; Cotrufo, M.F. Conceptualizing soil organic matter into particulate and mineral-associated forms to address global change in the 21st century. *Glob. Change Biol.* **2020**, *26*, 261–273. [CrossRef] [PubMed]
9. Yuan, X.; Qin, W.; Xu, H.; Zhang, Z.; Zhou, H.; Zhu, B. Sensitivity of soil carbon dynamics to nitrogen and phosphorus enrichment in an alpine meadow. *Soil Biol. Biochem.* **2020**, *150*, 107984. [CrossRef]
10. Sokol, N.W.; Sanderman, J.; Bradford, M.A. Pathways of mineral-associated soil organic matter formation: Integrating the role of plant carbon source, chemistry, and point of entry. *Glob. Change Biol.* **2019**, *25*, 12–24. [CrossRef] [PubMed]
11. Angst, G.; Mueller, K.E.; Nierop, K.G.; Simpson, M.J. Plant-or microbial-derived? A review on the molecular composition of stabilized soil organic matter. *Soil Biol. Biochem.* **2021**, *156*, 108189. [CrossRef]
12. Averill, C.; Waring, B. Nitrogen limitation of decomposition and decay: How can it occur? *Glob. Change Biol.* **2018**, *24*, 1417–1427. [CrossRef] [PubMed]
13. Yu, W.; Huang, W.; Weintraub-Leff, S.R.; Hall, S.J. Where and why do particulate organic matter (POM) and mineral-associated organic matter (MAOM) differ among diverse soils? *Soil Biol. Biochem.* **2022**, *172*, 108756. [CrossRef]
14. Neubauer, D.; Kolmakova, O.; Woodhouse, J.; Taube, R.; Mangelsdorf, K.; Gladyshev, M.; Premke, K.; Grossart, H. Zooplankton carcasses stimulate microbial turnover of allochthonous particulate organic matter. *ISME J.* **2021**, *15*, 1735–1750. [CrossRef]
15. Witzgall, K.; Vidal, A.; Schubert, D.I.; Höschen, C.; Schweizer, S.A.; Buegger, F.; Pouteau, V.; Chenu, C.; Mueller, C.W. Particulate organic matter as a functional soil component for persistent soil organic carbon. *Nat. Commun.* **2021**, *12*, 4115. [CrossRef]
16. Dorodnikov, M.; Kuzyakov, Y.; Fangmeier, A.; Wiesenberg, G.L.B. C and N in soil organic matter density fractions under elevated CO_2: Turnover vs. stabilization. *Soil Biol. Biochem.* **2011**, *43*, 579–589. [CrossRef]
17. Midwood, A.J.; Hannam, K.D.; Gebretsadikan, T.; Emde, D.; Jones, M.D. Storage of soil carbon as particulate and mineral associated organic matter in irrigated woody perennial crops. *Geoderma* **2021**, *403*, 115185. [CrossRef]
18. Chen, X.; Hu, Y.; Xia, Y.; Zheng, S.; Ma, C.; Rui, Y.; He, H.; Huang, D.; Zhang, Z.; Ge, T.; et al. Contrasting pathways of carbon sequestration in paddy and upland soils. *Glob. Change Biol.* **2021**, *27*, 2478–2490. [CrossRef]
19. Córdova, S.C.; Olk, D.C.; Dietzel, R.N.; Mueller, K.E.; Archontouilis, S.V.; Castellano, M.J. Plant litter quality affects the accumulation rate, composition, and stability of mineral-associated soil organic matter. *Soil Biol. Biochem.* **2018**, *125*, 115–124. [CrossRef]
20. Luan, L.; Jiang, Y.; Cheng, M.; Dini-Andreote, F.; Sui, Y.; Xu, Q.; Geisen, s.; Sun, B. Organism body size structures the soil microbial and nematode community assembly at a continental and global scale. *Nat. Commun.* **2020**, *11*, 6406. [CrossRef]
21. Lapidus, A.L.; Korobeynikov, A.I. Metagenomic data assembly–the way of decoding unknown microorganisms. *Front. Microbiol.* **2021**, *12*, 613791. [CrossRef] [PubMed]
22. Levkovich, S.A.; Gazit, E.; Bar-Yosef, D.L. Two decades of studying functional amyloids in microorganisms. *Trends Microbiol.* **2021**, *29*, 251–265. [CrossRef] [PubMed]
23. Laurent, J.M.; Jain, A.; Kan, A.; Steinacher, M.; Enrriquez Casimiro, N.; Stavrakis, S.; deMello, A.J.; Studart, A.R. Directed evolution of material-producing microorganisms. *Proc. Natl. Acad. Sci. USA* **2024**, *121*, e2403585121. [CrossRef] [PubMed]
24. Zhang, P.; Guan, P.; Hao, C.; Yang, J.; Xie, Z.; Wu, D. Changes in assembly processes of soil microbial communities in forest-to-cropland conversion in Changbai Mountains, northeastern China. *Sci. Total Environ.* **2022**, *818*, 151738. [CrossRef] [PubMed]

25. Shi, J.; Deng, L.; Gunina, A.; Alharbi, S.; Wang, K.; Li, J.; Liu, Y.; Shangguan, Z.; Kuzyakov, Y. Carbon stabilization pathways in soil aggregates during long-term forest succession: Implications from δ13C signatures. *Soil Biol. Biochem.* **2023**, *180*, 108988. [CrossRef]
26. Zhang, Q.; Wang, X.; Zhang, Z.; Liu, H.; Liu, Y.; Feng, Y.; Yang, G.; Ren, C.; Han, X. Linking soil bacterial community assembly with the composition of organic carbon during forest succession. *Soil Biol. Biochem.* **2022**, *173*, 108790. [CrossRef]
27. Liu, L.; Zhu, K.; Krause, S.M.; Li, S.; Wang, X.; Zhang, Z.; Shen, M.; Yang, Q.; Lian, J.; Wang, X.; et al. Changes in assembly processes of soil microbial communities during secondary succession in two subtropical forests. *Soil Biol. Biochem.* **2021**, *154*, 108144. [CrossRef]
28. Nemergut, D.R.; Schmidt, S.K.; Fukami, T.; O'Neill, S.P.; Bilinski, T.M.; Stanish, L.F.; Knelman, J.E.; Darcy, J.L.; Lynch, R.C.; Wickey, P.; et al. Patterns and processes of microbial community assembly. *Microbiol. Mol. Biol. Rev.* **2013**, *77*, 342–356. [CrossRef] [PubMed]
29. Luan, L.; Liang, C.; Chen, L.; Wang, H.; Xu, Q.; Jiang, Y.; Sun, B. Coupling bacterial community assembly to microbial metabolism across soil profiles. *mSystems* **2020**, *5*, e00298-20. [CrossRef]
30. Zhong, Y.; Sorensen, P.O.; Zhu, G.; Jia, X.; Liu, J.; Shangguan, Z.; Wang, R.; Yan, W. Differential microbial assembly processes and co-occurrence networks in the soil-root continuum along an environmental gradient. *iMeta* **2022**, *1*, e18. [CrossRef] [PubMed]
31. Yan, G.; Luo, X.; Huang, B.; Wang, H.; Sun, X.; Gao, H.; Zhou, M.; Xing, Y.; Wang, Q. Assembly processes, driving factors, and shifts in soil microbial communities across secondary forest succession. *Land Degrad. Dev.* **2023**, *34*, 3130–3143. [CrossRef]
32. Gibson, L.; Lee, T.M.; Koh, L.P.; Brook, B.W.; Gardner, T.A.; Barlow, J.; Peres, C.A.; Bradshaw, C.J.A.; Laurance, W.F.; Lovejoy, T.E.; et al. Primary forests are irreplaceable for sustaining tropical biodiversity. *Nature* **2011**, *478*, 378–381. [CrossRef] [PubMed]
33. Shao, P.; Liang, C.; Rubert-Nason, K.; Li, X.; Xie, H.; Bao, X. Secondary successional forests undergo tightly-coupled changes in soil microbial community structure and soil organic matter. *Soil Biol. Biochem.* **2019**, *128*, 56–65. [CrossRef]
34. Wang, S.; Wang, M.; Gao, X.; Zhao, W.; Miao, P.; Liu, Y.; Li, M.H. The diversity and composition of soil microbial communities differ in three land use types of the Sanjiang Plain, Northeastern China. *Microorganisms* **2024**, *12*, 780. [CrossRef]
35. Jenkinson, D.S.; Brookes, P.C.; Powlson, D.S. Measuring soil microbial biomass. *Soil Biol. Biochem.* **2004**, *36*, 5–7. [CrossRef]
36. Sinsabaugh, R.L.; Lauber, C.L.; Weintraub, M.N.; Ahmed, B.; Allison, S.D.; Crenshaw, C.; Contosta, A.R.; Cusack, D.; Frey, S.; Gallo, M.E.; et al. Stoichiometry of soil enzyme activity at global scale. *Ecol. Lett.* **2008**, *11*, 1252–1264. [CrossRef] [PubMed]
37. Yeates, C.; Gillings, M.R.; Davison, A.D.; Altavilla, N.; Veal, D.A. Methods for microbial DNA extraction from soil for PCR amplification. *Biol. Proced. Online* **1998**, *1*, 40–47. [CrossRef]
38. Quast, C.; Pruesse, E.; Yilmaz, P.; Gerken, J.; Schweer, T.; Yarza, P.; Peplies, J.; Glöckner, F.O. The SILVA ribosomal RNA gene database project: Improved data processing and web-based tools. *Nucleic Acids Res.* **2012**, *41*, D590–D596. [CrossRef] [PubMed]
39. Mori, A.S.; Fujii, S.; Kitagawa, R.; Koide, D. Null model approaches to evaluating the relative role of different assembly processes in shaping ecological communities. *Oecologia* **2015**, *178*, 261–273. [CrossRef] [PubMed]
40. Stegen, J.C.; Lin, X.; Konopka, A.E.; Fredrickson, J.K. Stochastic and deterministic assembly processes in subsurface microbial communities. *ISME J.* **2012**, *6*, 1653–1664. [CrossRef] [PubMed]
41. Avila-Jimenez, M.L.; Burns, G.; He, Z.; Zhou, J.; Hodson, A.; Avila-Jimenez, J.L.; Pearce, D. Functional associations and resilience in microbial communities. *Microorganisms* **2020**, *8*, 951. [CrossRef] [PubMed]
42. Wen, T.; Xie, P.; Yang, S.; Niu, G.; Liu, X.; Ding, Z.; Xue, C.; Liu, Y.; Shen, Q.; Yuan, J. ggClusterNet: An R package for microbiome network analysis and modularity-based multiple network layouts. *iMeta* **2022**, *1*, e32. [CrossRef] [PubMed]
43. Duan, L.; Li, J.L.; Yin, L.Z.; Luo, X.Q.; Ahmad, M.; Fang, B.Z.; Li, S.; Deng, Q.; Wang, P.; Li, W. Habitat-dependent prokaryotic microbial community, potential keystone species, and network complexity in a subtropical estuary. *Environ. Res.* **2022**, *212*, 113376. [CrossRef] [PubMed]
44. Peschel, S.; Müller, C.L.; Von Mutius, E.; Boulesteix, A.L.; Depner, M. NetCoMi: Network construction and comparison for microbiome data in R. *Brief. Bioinform.* **2021**, *22*, bbaa290. [CrossRef] [PubMed]
45. Ma, B.; Wang, H.; Dsouza, M.; Lou, J.; He, Y.; Dai, Z.; Brookes, P.C.; Xu, J.; Gilbert, J.A. Geographic patterns of co-occurrence network topological features for soil microbiota at continental scale in eastern China. *ISME J.* **2016**, *10*, 1891–1901. [CrossRef] [PubMed]
46. Lê Cao, K.A.; Welham, Z.M. *Multivariate Data Integration Using R: Methods and Applications with the Mixomics Package*; Chapman and Hall/CRC: Boca Raton, FL, USA, 2021. [CrossRef]
47. Oksanen, J.; Blanchet, F.G.; Kindt, R.; Legendre, P.; Minchin, P.R.; O'hara, B.; Simpson, G.L.; Solymos, P.; Stevens, H.; Wagner, H.H. Vegan: Community Ecology Package, Version 2.6–8. Available online: http://CRAN.R-project.org/package=vegan (accessed on 1 January 2024).
48. Lai, J.; Lortie, C.J.; Muenchen, R.A.; Yang, J.; Ma, K. Evaluating the popularity of R in ecology. *Ecosphere* **2019**, *10*, e02567. [CrossRef]
49. Costa, D.; Tavares, R.M.; Baptista, P.; Lino-Neto, T. The influence of bioclimate on soil microbial communities of cork oak. *BMC Microbiol.* **2022**, *22*, 163. [CrossRef]

50. Cotrufo, M.F.; Haddix, M.L.; Kroeger, M.E.; Stewart, C.E. The role of plant input physical-chemical properties, and microbial and soil chemical diversity on the formation of particulate and mineral-associated organic matter. *Soil Biol. Biochem.* **2022**, *168*, 108648. [CrossRef]
51. Poeplau, C.; Don, A.; Six, J.; Kaiser, M.; Benbi, D.; Chenu, C.; Cotrufo, M.F.; Derrien, D.; Gioacchini, P.; Grand, S.; et al. Isolating organic carbon fractions with varying turnover rates in temperate agricultural soils–A comprehensive method comparison. *Soil Biol. Biochem.* **2018**, *125*, 10–26. [CrossRef]
52. Luo, Y.; Xiao, M.; Yuan, H.; Liang, C.; Zhu, Z.; Xu, J.; Kuzyakov, Y.; Wu, J.; Ge, T.; Tang, C. Rice rhizodeposition promotes the build-up of organic carbon in soil via fungal necromass. *Soil Biol. Biochem.* **2021**, *160*, 108345. [CrossRef]
53. Six, J.; Callewaert, P.; Lenders, S.; De Gryze, S.; Morris, S.J.; Gregorich, E.G.; Paul, E.A.; Paustian, K. Measuring and understanding carbon storage in afforested soils by physical fractionation. *Soil Sci. Soc. Am. J.* **2002**, *66*, 1981–1987. [CrossRef]
54. Garcia-Franco, N.; Martínez-Mena, M.; Goberna, M.; Albaladejo, J. Changes in soil aggregation and microbial community structure control carbon sequestration after afforestation of semiarid shrublands. *Soil Biol. Biochem.* **2015**, *87*, 110–121. [CrossRef]
55. An, S.; Mentler, A.; Mayer, H.; Blum, W.E. Soil aggregation, aggregate stability, organic carbon and nitrogen in different soil aggregate fractions under forest and shrub vegetation on the Loess Plateau, China. *Catena* **2010**, *81*, 226–233. [CrossRef]
56. Ye, C.; Chen, D.; Hall, S.J.; Pan, S.; Yan, X.; Bai, T.; Guo, H.; Zhang, Y.; Bai, Y.; Hu, S. Reconciling multiple impacts of nitrogen enrichment on soil carbon: Plant, microbial and geochemical controls. *Ecol. Lett.* **2018**, *21*, 1162–1173. [CrossRef] [PubMed]
57. Hu, P.; Zhang, W.; Chen, H.; Li, D.; Zhao, Y.; Zhao, J.; Xiao, J.; Wu, F.; He, X.; Luo, Y.; et al. Soil carbon accumulation with increasing temperature under both managed and natural vegetation restoration in calcareous soils. *Sci. Total Environ.* **2021**, *767*, 145298. [CrossRef]
58. Shi, J.; Yang, L.; Liao, Y.; Li, J.; Jiao, S.; Shangguan, Z.; Deng, L. Soil labile organic carbon fractions mediate microbial community assembly processes during long-term vegetation succession in a semiarid region. *iMeta* **2023**, *2*, e142. [CrossRef]
59. Barberán, A.; Bates, S.T.; Casamayor, E.O.; Fierer, N. Using network analysis to explore co-occurrence patterns in soil microbial communities. *ISME J.* **2012**, *6*, 343–351. [CrossRef] [PubMed]
60. Graham, E.B.; Knelman, J.E. Implications of soil microbial community assembly for ecosystem restoration: Patterns, process, and potential. *Microb. Ecol.* **2023**, *85*, 809–819. [CrossRef]
61. Kang, H.; Xue, Y.; Cui, Y.; Moorhead, D.L.; Lambers, H.; Wang, D. Nutrient limitation mediates soil microbial community structure and stability in forest restoration. *Sci. Total Environ.* **2024**, *935*, 173266. [CrossRef] [PubMed]
62. Anthony, M.A.; Crowther, T.W.; Maynard, D.S.; van den Hoogen, J.; Averill, C. Distinct assembly processes and microbial communities constrain soil organic carbon formation. *One Earth* **2020**, *2*, 349–360. [CrossRef]
63. Osburn, E.D.; Aylward, F.O.; Barrett, J.E. Historical land use has long-term effects on microbial community assembly processes in forest soils. *ISME Commun.* **2021**, *1*, 48. [CrossRef] [PubMed]
64. Liu, W.; Graham, E.B.; Zhong, L.; Zhang, J.; Li, W.; Li, Z.; Lin, X.; Feng, Y. Dynamic microbial assembly processes correspond to soil fertility in sustainable paddy agroecosystems. *Funct. Ecol.* **2020**, *34*, 1244–1256. [CrossRef]
65. Gao, G.F.; Peng, D.; Tripathi, B.M.; Zhang, Y.; Chu, H. Distinct community assembly processes of abundant and rare soil bacteria in coastal wetlands along an inundation gradient. *mSystems* **2020**, *5*, e01150-20. [CrossRef]
66. Zhao, Z.; Ma, Y.; Feng, T.; Kong, X.; Wang, Z.; Zheng, W.; Zhai, B. Assembly processes of abundant and rare microbial communities in orchard soil under a cover crop at different periods. *Geoderma* **2022**, *406*, 115543. [CrossRef]
67. Ni, Y.; Yang, T.; Ma, Y.; Zhang, K.; Soltis, P.S.; Soltis, D.E.; Gilbert, J.A.; Zhao, Y.; Fu, C.; Chu, H. Soil pH determines bacterial distribution and assembly processes in natural mountain forests of eastern China. *Glob. Ecol. Biogeogr.* **2021**, *30*, 2164–2177. [CrossRef]
68. Li, W.; Kuzyakov, Y.; Zheng, Y.; Li, P.; Li, G.; Liu, M.; Alharbi, H.A.; Li, Z. Depth effects on bacterial community assembly processes in paddy soils. *Soil Biol. Biochem.* **2022**, *165*, 108517. [CrossRef]
69. Romdhane, S.; Spor, A.; Aubert, J.; Bru, D.; Breuil, M.C.; Hallin, S.; Mounier, A.; Ouadah, S.; Tsiknia, M.; Philippot, L. Unraveling negative biotic interactions determining soil microbial community assembly and functioning. *ISME J.* **2022**, *16*, 296–306. [CrossRef] [PubMed]
70. Liao, H.; Hao, X.; Zhang, Y.; Qin, F.; Xu, M.; Cai, P.; Chen, W.; Huang, Q. Soil aggregate modulates microbial ecological adaptations and community assemblies in agricultural soils. *Soil Biol. Biochem.* **2022**, *172*, 108769. [CrossRef]
71. Zheng, T.; Xie, H.; Thompson, G.L.; Bao, X.; Deng, F.; Yan, E.; Zhou, X.; Liang, C. Shifts in microbial metabolic pathway for soil carbon accumulation along subtropical forest succession. *Soil Biol. Biochem.* **2021**, *160*, 108335. [CrossRef]
72. Dong, L.; Li, J.; Liu, Y.; Hai, X.; Li, M.; Wu, J.; Wang, X.; Shangguan, Z.; Zhou, Z.; Deng, L. Forestation delivers significantly more effective results in soil C and N sequestrations than natural succession on badly degraded areas: Evidence from the Central Loess Plateau case. *Catena* **2022**, *208*, 105734. [CrossRef]
73. Teixeira, H.M.; Cardoso, I.M.; Bianchi, F.J.; da Cruz Silva, A.; Jamme, D.; Peña-Claros, M. Linking vegetation and soil functions during secondary forest succession in the Atlantic forest. *For. Ecol. Manag.* **2020**, *457*, 117696. [CrossRef]

74. Arunrat, N.; Sansupa, C.; Sereenonchai, S.; Hatano, R.; Lal, R. Fire-induced changes in soil properties and bacterial communities in rotational shifting cultivation fields in Northern Thailand. *Biology* **2024**, *13*, 383. [CrossRef] [PubMed]
75. Jiao, S.; Chu, H.; Zhang, B.; Wei, X.; Chen, W.; Wei, G. Linking soil fungi to bacterial community assembly in arid ecosystems. *iMeta* **2022**, *1*, e2. [CrossRef] [PubMed]